

Transport properties of $L_{1-x}\text{Sr}_x\text{MnO}_3$ ($L=\text{Pr}, \text{Nd}$; $\frac{1}{4}\leq x\leq\frac{1}{2}$)

B. Fisher, L. Patlagan, and G. M. Reisner

Physics Department and Crown Center for Superconductivity, Technion, Haifa, Israel 32000

(Received 21 May 1996)

We report on the temperature dependence of the zero-field resistivity (ρ), absolute thermopower (S) and the room temperature lattice constants of the title materials. The results indicate that at high temperatures, above the transition to the ferromagnetic (FM) state electronic transport is carried out in narrow bands. An attempt to account for the measured values of S was put forward. Evidence for the presence of a gap in the density of states of the compounds with $x\sim\frac{1}{4}$, possibly due to Coulomb repulsion, was found in $S(T)$ at temperatures far above T_c . The positive sign of S found in the FM state of most of the compounds studied is consistent with transport in a one-electron band with polarized states. The temperature dependence of the resistivity in the FM state is consistent with a transition probability which depends exponentially on the transfer integral. [S0163-1829(96)06438-7]

I. INTRODUCTION

A series of doped manganese oxides of the type $L_{1-x}A_x\text{MnO}_3$ ($L\text{AMnO}$, with L -lanthanide, A -alkaline ions) undergo, upon cooling, a transition from a paramagnetic (PM) state to a ferromagnetic (FM) state accompanied by a change from a negative to a positive temperature coefficient (ntc to ptc) of the zero-field resistivity- ρ . In terms of the double-exchange model,^{1,2} the itinerant holes, created by the substitution of L^{3+} by A^{2+} ions, provide the FM interaction. The number of holes per formula unit is identified with the concentration of tetravalent Mn which is taken equal to x .³ The temperature T_m of the resistivity maximum ρ_m is identified with the transition to the FM state⁴ ($T_m\sim T_c$). The strong dependence of the resistivity on magnetization and thus on the applied magnetic field- H , leads to giant negative magnetoresistance (GMR), also called *colossal magnetoresistance* (CMR). The discovery of this effect,⁵ with its applicative implications, has revived interest in these materials. The response to the magnetic field is maximal around T_m .⁴ For a given (L,A) pair T_m is maximal at an optimal A concentration, x_c , typically around $\frac{1}{3}$. For a given alkaline ion at fixed concentration around x_c , T_m increases strongly with the average lanthanide ionic radius $\langle r \rangle$.^{6,7} Application of hydrostatic pressure has a similar effect on T_m as increasing $\langle r \rangle$.⁸ An anomalous thermal expansion is found around T_m .⁹ These effects demonstrate the strong electron-lattice interaction in these materials.

A first-order transition from the FM state to a low-temperature charge-ordered antiferromagnetic (CO-AFM) state was observed in $\text{Pr}_{1-x}\text{Sr}_x\text{MnO}_3$ around $x=\frac{1}{2}$.¹⁰ It is accompanied by a large increase of the resistivity and a change from ptc to ntc of ρ . The onset of the CO-AFM state is believed to be driven by the Coulomb repulsion between the charge carriers and is optimized when the carrier concentration is commensurate with the lattice periodicity. In $\text{Pr}_{1-x}\text{Ca}_x\text{MnO}_3$,^{11,12} which is nonmetallic for all x , the CO-AFM state persists for a wide range of x . The collapse of the CO state under magnetic fields leads also to CMR.

The dramatic changes in resistivity accompanying the transition from the PM to FM state, or from the FM to AFM

state (for $x\sim\frac{1}{2}$), are frequently regarded as insulator-metal or metal-insulator transitions, respectively. These materials are poor conductors even in the FM state and as suggested in Ref. 4 the electronic transport process in this state cannot be regarded as metalliclike; these authors reached the conclusion that polaronic hopping is the prevalent conduction mechanism both above and below T_c .

The temperature dependence of the absolute thermopower (S) is a very sensitive probe of the electronic structure of conductors around E_f and a powerful indicator of phase transitions of various types. It is particularly useful in studying the band-filling and the correlations between charge carriers when electronic transport is carried out in narrow bands. It was measured 35 years ago on the LaCaMnO system¹³ for the whole range of compositions $0\leq x\leq 1$,¹⁴ for several samples it was measured up to ~ 1400 K. Observation of giant magnetothermal effects accompanying GMR in LaSrMnO crystals¹⁵ ($0.15\leq x\leq 0.5$) and LaCaMnO films¹⁶ ($x=\frac{1}{3}$) were recently reported. We used this technique combined with zero-field resistivity measurements in studying $\text{Nd}_{1-x}\text{Sr}_x\text{MnO}_3$ and $\text{Pr}_{1-x}\text{Sr}_x\text{MnO}_3$ with $\frac{1}{4}\leq x\leq\frac{1}{2}$. These systems were chosen because they exhibit all the phenomena mentioned above at very convenient temperatures, e.g., T_m and T_v are below room temperature (RT). We also determined the RT lattice constants of samples of the various compositions.

II. EXPERIMENT

We prepared polycrystalline samples of $L_{1-x}\text{Sr}_x\text{MnO}_3$ ($L=\text{Pr}, \text{Nd}$; $\frac{1}{4}\leq x\leq\frac{1}{2}$) by the standard solid-state reaction, very similar to that used by the authors of Ref. 17 for the preparation of targets for epitaxial films. The last anneal (in air) was at 1470°C .

The resistance of the samples was measured in a closed cycle refrigerator, working from room-temperature (RT) down to 10 K. The thermopower measurements were performed in a cryostat working from 400 K down to liquid nitrogen temperature (LNT). The reproducibility of the results, checked by repeated measurements on several samples,

TABLE I. Composition and room temperature crystallographic lattice constants.

Pr _{1-x} Sr _x MnO ₃				Nd _{1-x} Sr _x MnO ₃				
x (Sr)	$\frac{1}{4}$	$\frac{1}{3}$	$\frac{1}{2}$	$\frac{1}{4}$	$\frac{2}{7}$	$\frac{1}{3}$	$\frac{2}{5}$	$\frac{1}{2}$
a (Å)	5.474(1)	5.484(2)	5.404(1)	5.465(1)	5.460(1)	5.451(1)	5.471(2)	5.473(1)
b (Å)		5.455(2)					5.437(2)	5.430(1)
c (Å)	7.747(2)	7.709(3)	7.789(2)	7.724(2)	7.717(1)	7.716(2)	7.678(2)	7.626(2)
V (Å ³)	232.14	230.62	227.46	230.69	230.06	229.27	228.39	226.63

over complete, or over portions of temperature cycles, was found to be very good.

All samples were characterized by x-ray powder diffraction (Siemens D-5000 diffractometer, CuK α radiation). The lattice parameters were determined by least-squares fitting of reflection peaks in the range $6^\circ \leq 2\theta \leq 140^\circ$ (0.02° per 8 sec. step). All lines of x-ray patterns could be indexed in terms of the lattices shown in Table I, thus confirming that the samples were of single phase.

III. EXPERIMENTAL RESULTS

The RT unit cell volume (V) as a function of Sr content x is plotted in Fig. 1. The unit cells contain four formula units. For both NdSrMnO and PrSrMnO, V drops linearly with x . The line for PrSrMnO (with the larger $r(L)$) lies higher and its slope is steeper than that for NdSrMnO.

Figure 2(a) shows the temperature dependence of the resistivity ρ and Fig. 2(b) shows the absolute thermopower S for Nd_{1-x}Sr_xMnO₃ samples. Corresponding results for Pr_{1-x}Sr_xMnO₃ are shown in Fig. 3. The dashed lines in Fig. 3(b) represent the data for Nd_{1-x}Sr_xMnO₃ samples with $x = \frac{1}{4}, \frac{1}{3},$ and $\frac{1}{2}$, replotted there for comparison.

As seen in Fig. 2(a), each plot of $\rho(T)$ for Nd_{1-x}Sr_xMnO₃ has a maximum $\rho_m(x)$ at $T_m(x)$; ρ_m increases with decreasing x and T_m is the highest for $x=0.4$. Around T_m , $\rho(T)$ is very asymmetric for $\frac{1}{3} \leq x \leq \frac{1}{2}$ (note the weak dependence of ρ on T above T_m , and the strong dependence on T below T_m), and becomes remarkably symmetric for $x = \frac{1}{4}$. Straight lines could be traced on the semilog plots of ρ vs T for $x = \frac{1}{4}$ on both sides of T_m . They represent $\rho = \rho_0 \exp(\alpha T)$, with α positive below T_m and negative above T_m . Each of these two lines fit the data points on both sides of T_m for almost one

order of magnitude of ρ . Straight lines with smaller (positive) slopes and lower extrapolated values (ρ_0) at $T=0$ were traced also through data points lying below T_m on the plots for $x \geq \frac{2}{5}$. The slopes of the straight lines, $d \ln \rho / dT = \alpha$ are shown on the graphs. For $x = \frac{1}{4}$, the data points at $T \sim T_m$ fall on a rounded tip of the cusp. For the following three compositions the data points around T_m stick out, far above the straight lines. At low temperatures the data points deviate gradually from the straight line towards a saturation value reached around 50 K. A small deviation from the straight line is observed for the data points for $x = \frac{1}{4}$ close to RT. For $x = \frac{1}{2}$, a narrow range of ρ with ptc is followed at lower

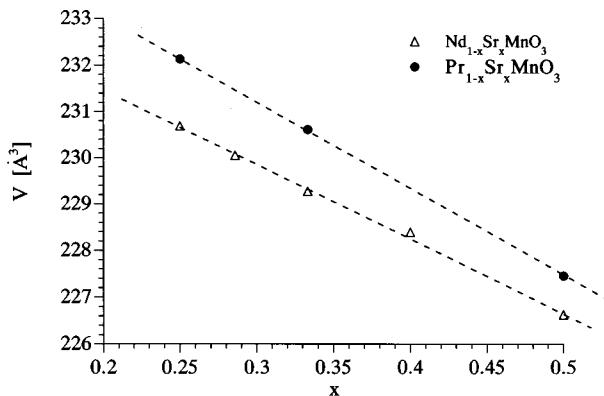
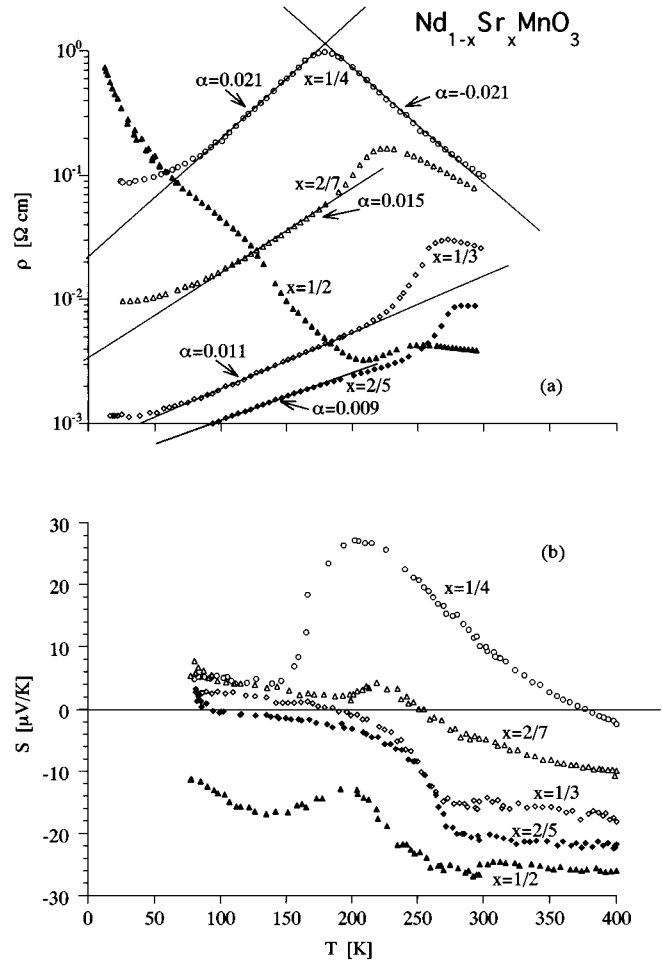
FIG. 1. Room temperature unit cell volume vs x .

FIG. 2. Resistivity $\rho(a)$ and absolute thermopower $S(b)$ vs T for samples of Nd_{1-x}Sr_xMnO₃ at various values of x . The straight lines represent $\rho = \rho_0 \exp(\alpha T)$. The values of α are given in the figure.

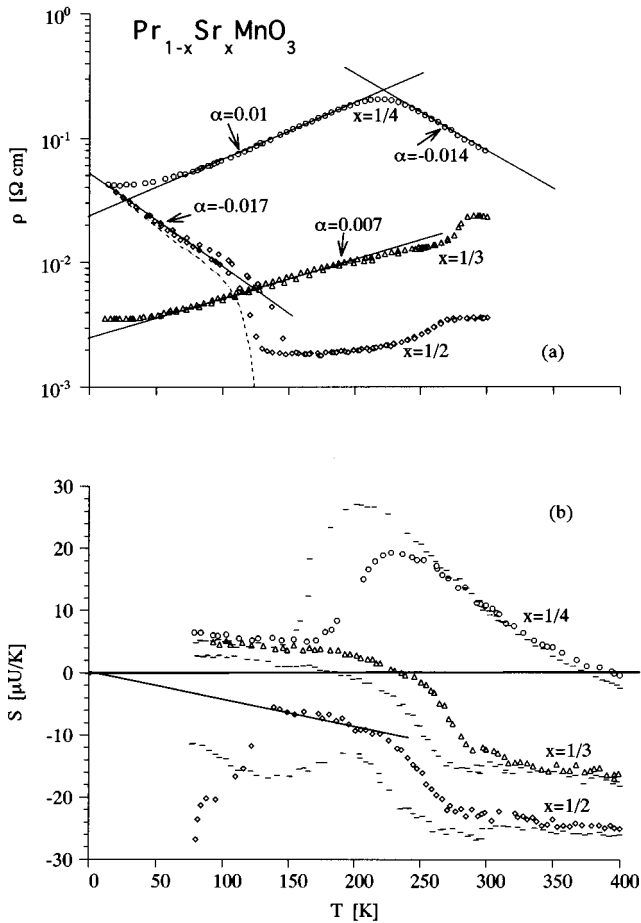


FIG. 3. Resistivity $\rho(a)$ and absolute thermopower $S(b)$ vs T for samples of $\text{Pr}_{1-x}\text{Sr}_x\text{MnO}_3$ at various values of x . (a) The straight lines represent $\rho = \rho_0 \exp(\alpha T)$. The values of α are given in the figure. The dashed line below the low-temperature data for $x = \frac{1}{2}$ was obtained by subtracting the minimal resistivity from the ρ data. (b) The straight solid line represents $S = -0.04T \mu\text{V/K}$. $(-S(T))$ for $\text{Nd}_{1-x}\text{Sr}_x\text{MnO}_3$ with $x = \frac{1}{2}, \frac{1}{3}$, and $\frac{1}{4}$ replotted here for comparison.

temperatures by ρ with *ntc*. This latter feature is identified with the transition to the CO-AFM state¹⁸ which is not well resolved in our samples with $L=\text{Nd}$.

The plots of $\rho(T)$ for $L=\text{Pr}$ [see Fig. 3(a)] exhibit with few exceptions the features of the corresponding plots for $L=\text{Nd}$. The values of T_m are higher and those of ρ_m are lower [for this comparison see Figs. 4(a) and 4(b)]. The absolute values of α are also lower. For $x = \frac{1}{3}$, the steep rise towards ρ_m is preceded by a weak dependence of ρ on T (the points lie below the straight line). For $x = \frac{1}{2}$, T_m may be identified with the change in the slope of $\rho(T)$ because in the narrow range up to RT ρ is almost constant.

The first-order transition to the CO-AFM state at T_v (Ref. 10) is exhibited in our plot for $\text{Pr}_{0.5}\text{Sr}_{0.5}\text{MnO}_3$ by a jump to high ρ with *ptc* and hysteresis. The transition temperatures T_m and T_v are similar to those in Ref. 10 for a single crystal but the transitions in our samples are less sharp and ρ varies very little with temperature between the two transitions. As is often observed in structural phase transitions, our $\text{Pr}_{0.5}\text{Sr}_{0.5}\text{MnO}_3$ samples exhibited irreversibilities. Following one cooling-heating cycle through T_v , $\rho(\text{RT})$ changed by

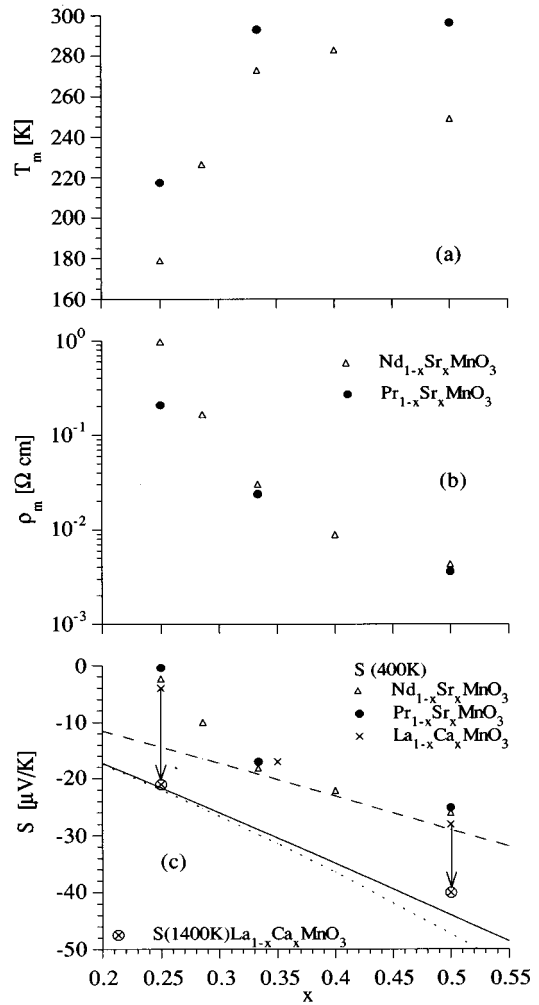


FIG. 4. T_m (a), ρ_m (b), and S (400 K) (c) vs x for $\text{Nd}_{1-x}\text{Sr}_x\text{MnO}_3$ and $\text{Pr}_{1-x}\text{Sr}_x\text{MnO}_3$. The data for $\text{La}_{1-x}\text{Ca}_x\text{MnO}_3$ at 400 and 1400 K were taken from Ref. 13. $S_{\text{sat}} = (k_B/|e|) \ln[(1-x/a)/(1+x/a)]$ is represented by the dashed line for $a=3$, and by the solid line for $a=2$. The dotted line represents calculated values of S_{sat} for bipolarons.

$\sim \pm 0.5 \text{ m}\Omega \text{ cm}$. The plot shown here represents the data taken after several full cooling-heating cycles, following which the resistivity became reversible at the expense of a net increase with respect to its initial value. It is possible that the values of $\rho(x = \frac{1}{2})$ measured between T_c and T_v do not represent the bulk but a residual resistivity of macroscopic defects. The dashed line traced for $T < T_v$ was obtained after subtracting the minimal resistivity (above T_v) from the $\rho(T)$ data obtained during the cooling portion of the cycle. It is seen that this procedure does not affect much the results in the low- T regime. Both the corrected and the original data points lie on an almost straight line with slightly different slopes. It is notable that the (negative) α so obtained is comparable with that obtained for $x = \frac{1}{4}$ above T_m . A similar exponential drop of ρ with T can be seen in Fig. 2 of Ref. 10 for the single crystal of $\text{Pr}_{0.5}\text{Sr}_{0.5}\text{MnO}_3$ in the lowest temperature regime.

From the plots of S vs T [Figs. 2(b) and 3(b)] it is seen that there is very little difference between the data for the $L=\text{Nd}$ and $L=\text{Pr}$ samples with the same x . Our plots are

very similar to those published previously for $\text{La}_{1-x}\text{Ca}_x\text{MnO}_3$, in the overlapping ranges of x and T .¹³ There is also a qualitative agreement between our results and those shown in Ref. 15 for $\text{La}_{1-x}\text{Ca}_x\text{MnO}_3$ in the temperature range $T \leq T_m$ (For the samples discussed in Ref. 15, T_m is above RT).

For $\frac{1}{2} \leq x \leq \frac{1}{3}$ and $T > T_m$, S is negative, almost independent on temperature and increases (becomes less negative) with decreasing x . For these compositions, the transition to the FM state is marked by steep rises of S towards zero. The pair of plots for the two different L and same x separate at the higher T_m . [For a given x , $T_m(\text{Nd}) < T_m(\text{Pr})$.] For $x \leq 0.4$ these rises are followed at $T < T_m$ by saturation at zero or low positive values.

For the two lowest values of x ($\frac{2}{7}$ and $\frac{1}{4}$), $S(T_m < T < 400 \text{ K})$ is not constant but rises with decreasing temperature. A sign reversal occurs far above T_m . With lowering T , S reaches a positive maximum (S_m) followed by a rather sharp drop towards low positive saturation values at lower T .

For $x \leq 0.4$ and both L , all $S(T)$ plots group below the FM transition region around constant, small positive values (close to zero). In this regime our results are close to those found in Ref. 16 for $\text{La}_{0.66}\text{Ca}_{0.33}\text{MnO}_3$. For $\text{Pr}_{0.5}\text{Sr}_{0.5}\text{MnO}_3$, $S(T < T_m)$ rises linearly towards zero. This rise is interrupted at T_v where S drops to large negative values. For the $\text{Nd}_{0.5}\text{Sr}_{0.5}\text{MnO}_3$ samples $S(T < T_m)$ is more complicated [see Fig. 3(b)]; this behavior, like that of its $\rho(T)$, is probably due to the proximity between the FM and AFM states.

IV. DISCUSSION

A. Resistivity

The values of ρ_m obtained in this work span over more than two orders of magnitude [see Fig. 4(b)] and the ntc (above T_m) increases with increasing ρ_m . Similar behavior was found in various magnetic alloys. In $(\text{Fe}_{1-x}\text{V}_x)_3\text{Si}$,¹⁹ it was found that the onset of ntc of ρ in the PM state occurs when the resistivities around T_c exceed $\sim 150 \mu\Omega \text{ cm}$. All our ρ_m exceed this value and the onset of ntc seems to correspond to a value of ρ_m about one order of magnitude higher. Large ntc are observed only when $\rho_m > 10^{-2} \Omega \text{ cm}$. These values exceed the Mott maximum metallic resistivity indicating that around T_m the carriers may be treated as localized with transport carried out via phonon assisted tunneling (hopping). Only for $x = \frac{1}{4}$ the temperature range of ntc of ρ is wide enough for quantitative analysis. Expressions of the type $\ln\rho \propto (T_0/T)^p$ for variable range hopping ($p \sim \frac{1}{4}$) or nearest-neighbor hopping with constant activation energy ($p = 1$) do not seem to fit the experimental data. In this temperature range the exponential drop of ρ with T fits them better. The same temperature dependence seems to fit best the results for the $\text{Pr}_{0.5}\text{Sr}_{0.5}\text{MnO}_3$ samples at $T < T_v$.²⁰ This regime can be seen also in the results for the single crystal without magnetic field, in the range $0 < T < 50 \text{ K}$ (see Fig. 2 in Ref. 10). Note that in our case the line that fits $\rho(T < T_v)$ for $\text{Pr}_{0.5}\text{Sr}_{0.5}\text{MnO}_3$ is almost parallel to the straight line on the graph for $\text{Pr}_{0.75}\text{Sr}_{0.25}\text{MnO}_3$ but shifted to lower values of the resistivity and temperatures. This suggests that the transport mechanisms above 250 K in the samples with $x = \frac{1}{4}$ and below 120 K in those with $x = \frac{1}{2}$ are similar. If this temperature dependence of ρ is typical for the AF state, it indicates

that the samples with $x = \frac{1}{4}$ may also be in the AF state for $T_m < T < RT$. An exponential drop of the resistivity with temperature has been observed in many systems,²¹ often over many orders of magnitude. In most cases this temperature dependence is followed at lower temperatures by an activated-type temperature dependence [as seems to be the case in $\rho(T < T_v)$ for $\text{Nd}_{0.5}\text{Sr}_{0.5}\text{MnO}_3$]. Its interpretation in terms of tunneling through a vibrating barrier²¹ is still under dispute.²²

The temperature dependence of ρ found in our FM samples, e.g., an exponential rise of ρ with T preceded by saturation at low temperatures, can be seen in many plots of $\ln(\rho)$ vs T for FM-LAMnO samples. It can be seen, for example, in Fig. 2 of Ref. 10 for the single crystal of $\text{Pr}_{0.5}\text{Sr}_{0.5}\text{MnO}_3$. Without magnetic field the temperature range of the linear dependence is narrow being limited by T_v . The range of temperatures of the linear portions of the graphs increases with increasing H . The characteristic shape of $\ln(\rho)$ vs T , in the FM state, including saturation of ρ at $T \rightarrow 0$ is fully recovered when the AF state is suppressed by a field of 70 KOe.

The strong dependence of ρ on x (for fixed T) cannot be accounted for by the variation in the band filling. The rise of $\ln(\rho)$ with decreasing x at fixed T seems to be correlated with the dependence of the unit cell volume with decreasing x . The plots of $\ln(\rho)$ vs T in the FM state, resemble typical plots of thermal expansion of solids.²³ The enhanced increase of ρ close to T_m for $x \geq \frac{1}{3}$ is probably related to the large magnetovolume effect found in related materials.⁹ The temperature dependence of ρ emphasizes the effect of Sr doping on the mobility of the carriers, e.g., on the transfer integral.

B. Thermopower

The most general formula for the absolute thermopower, holding for charge carriers in extended or localized states is²⁴

$$S = - \frac{1}{|e|T} \langle E - \mu \rangle, \quad (1)$$

where $\langle E - \mu \rangle$ is an average energy of the states participating in transport, measured from the chemical potential μ . For transport in a single band of width W , $|S|$ increases with temperature when $k_B T / W \ll 1$. For fixed population in a narrow band (NB) S approaches saturation when $k_B T \sim W$. The almost constant values of S observed at $T > T_m$ for each $\frac{1}{3} \leq x \leq \frac{1}{2}$ and its dependence on x , but not on the (LA) pair, support the possibility previously suggested in Ref. 13 that the band is narrow. The saturation value of S is

$$S_{\text{sat}} = \frac{k_B}{|e|} \ln \left(b \frac{n}{p} \right), \quad (2)$$

where n/p is the electron/hole ratio and b is the spin-degeneracy factor. ($b=1$ for nondegenerate states, $b=\frac{1}{2}$ for doubly degenerate states). The negative sign obtained for $T > T_m$ in the samples with $\frac{1}{3} \leq x \leq \frac{1}{2}$ is consistent with a population of uncorrelated electrons in a less-than-half filled band as proposed in Ref. 15, e.g., $n = 1 - x$, $p = 1 + x$ (each Sr ion contributes one hole to the NB) and $b=1$. However the values of S_{sat} obtained by these substitutions in Eq. (2) are far

more negative than those measured in this work at 400 K. For $x \geq \frac{1}{3}$ the discrepancy is about a factor of 3.

In Fig. 4(c) we plotted $S(400 \text{ K})$ for our samples and for the LaCaMnO samples from Ref. 13. We also added the two data points of $S(1400 \text{ K})$ available for the latter system in the relevant range of concentrations. The agreement between the results for $S(400 \text{ K})$ for the three systems both in the range of weak temperature dependence ($x \geq \frac{1}{3}$) and strong temperature dependence ($x = \frac{1}{4}$) is remarkable. The temperature dependence of $S(x \sim \frac{1}{4})$ with the sign reversal and the maximum in $S(T)$ (S_m) seen in our work is also very similar to that observed in Ref. 13. With decreasing x , $S_m(\text{LaCaMnO})$ shifts to lower temperatures and its magnitude increases. It is possible that $S(400 \text{ K})$ for $x \geq \frac{1}{3}$ cannot yet be considered as S_{sat} due to finite band effects. This argument does not hold for $S(1400 \text{ K})$; the data for LaCaMnO samples can be considered as saturation values of S because they are preceded by a wide range of constant S .

Several possibilities have been considered in order to account for the values of S of these materials measured at high temperatures. The simplest are discussed here. The dashed line in Fig. 4(c) represents calculated values of S_{sat} using Eq. (2) with $b=1$, $n/p=(1-x/a)/(1+x/a)$ and $a=3$. It lies close to the data for $\frac{1}{3} \leq x \leq \frac{1}{2}$ (for which the temperature dependence of S around 400 K is weak). The solid line represents values of S_{sat} calculated similarly as above with $a=2$. This line fits very well the two data for $S(1400 \text{ K})$ $\text{La}_{1-x}\text{Ca}_x\text{MnO}_3$. The numerical values may be obtained for either (1) a nondegenerate two-electron band filled with $1-x/a$ carriers, e.g., the number of holes created in the narrow band by the substitution of L^{3+} by A^{2+} ions is much smaller than x ($\Delta p = x/a$); or (2) a nondegenerate band with $2a$ states per formula unit filled with $a-x$ carriers ($\Delta p = x$). The first possibility (1) can be easily quantified by assuming that part of the holes reside in traps created by the doping.

A rather remote, but worth mentioning possibility (3) is represented by the dotted line in Fig. 4(c). It shows the calculated values of S_{sat} for bipolarons in a two-electron band. For the same population of electrons in such band (or narrow spread of states), the absolute thermopower of bipolarons is half of that obtained for polarons [e should be replaced by $2e$ in Eq. (2)]. It lies close to the solid line because for $\frac{1}{4} \leq x \leq \frac{1}{2}$, $\ln[(1-x/2)/(1+x/2)] \approx (1/2)\ln[(1-x)/(1+x)]$.

All three possibilities discussed above imply $S_{\text{sat}}=0$ for $n/p=1$ ($x=0$). And indeed this is the result shown in Ref. 13 for LaMnO_3 at $T > 1000 \text{ K}$.²⁵ More experimental data are needed in order to find out if one of them is reasonable. However, as shown below, the second possibility with $a=2$ can lead to a simple, quantitative interpretation of the temperature dependence of S for at least $x = \frac{1}{4}$.

Suppose that a gap Δ opens in the NB with four states per formula unit, splitting it into a lower band with three states and an upper band with one state per formula unit. For $T \ll \Delta/k_B T$ only the lower band will participate in transport. Using again Eq. (2) with $b=1$, $n=2-x$ and $p=1+x$ we obtain $S=29 \mu\text{V/K}$ for $x = \frac{1}{4}$. Within the experimental error this is exactly $S_m(\text{Nd}_{0.75}\text{Sr}_{0.25}\text{MnO}_3)$. It is worth noting that this model predicts $S \geq 0$ for $x \geq \frac{1}{2}$. It may represent the high-temperature precursor to the onset of magnetic order. Finite band effects and/or the transition to the FM state may cause

the reduction of S_m in $\text{Nd}_{0.71}\text{Sr}_{0.29}\text{MnO}_3$ and in $\text{Pr}_{0.75}\text{Sr}_{0.25}\text{MnO}_3$ from the maximal predicted value.

The temperature dependence of S obtained for $x \sim \frac{1}{4}$ around the temperature of the sign reversal may also be interpreted as the transition in a two-electron NB from nondegenerate to degenerate states, due to Coulomb repulsion.²⁶ In this case the sign reversals of S occur for $\frac{2}{3} < n < 1$ (or for $\frac{4}{3} < n < 2$) when the Coulomb energy U is of the order of $k_B T$. The NB values $S(U/k_B T \gg 1) = S_c$ can be obtained using Eq. (2) for $p=1-n$ and $b=\frac{1}{2}$. This yields $S_c=35 \mu\text{V/K}$ for $n=\frac{3}{4}$ ($x=\frac{1}{4}$). This is only slightly higher than $S_m(\text{Nd}_{0.75}\text{Sr}_{0.25}\text{MnO}_3)$. This is a very attractive model because it is consistent with the presently accepted picture of the electronic structure of LAMnO. Its weakness stems from the predicted S_{sat} which are much larger than the measured ones.

While the sign of S for $x < \frac{1}{2}$ in the FM state is well understood, a quantitative analysis of S in this state is difficult since it may be expected that $W/k_B T$ is large and dependent on temperature. The grouping of all $S(T)$ plots for $x \leq 0.4$ around small, constant values is remarkable in view of the resistivities of the materials which are of different orders of magnitudes [for $L=\text{Nd}$ at 150 K $\rho(1/4)/\rho(1/3) \approx 200!$].

In the narrow temperature range between T_v and T_m , $S(T)$ for $\text{Pr}_{0.5}\text{Sr}_{0.5}\text{MnO}_3$ exhibits a simple behavior; a line representing $S \approx -0.04T \mu\text{V/K}$ can be traced within the scatter of the data points. This would correspond to an S of a wide metallic band²⁷ with E_f estimated at a fraction of an eV. This however should not be taken too seriously in view of the proximity to the CO-AFM state and the peculiar behavior of $S(T)$ in the other FM compounds studied in this work. Measurements of $S(T)$ for $\text{Pr}_{0.5}\text{Sr}_{0.5}\text{MnO}_3$ under high magnetic fields, which would retain the FM state down to the lowest temperatures could provide the best test for such interpretation. It should be mentioned that in the ideal case (perfect stoichiometry, absence of hole traps and perfect symmetry of the band) $S(\text{FM-Pr}_{0.5}\text{Sr}_{0.5}\text{MnO}_3)$ should be zero, for arbitrary bandwidth.

V. CONCLUSIONS AND REMARKS

The results of thermopower measurements in the present work on the NdSrMnO and PrSrMnO systems and in an early work on the LaCaMnO system are consistent with transport in narrow bands. Three different scenarios that can account for the saturation values of S at high temperatures have been discussed. Common to all three is that the bands are less than half-filled for $x \leq 1$. The absolute values of the resistivities are consistent with carrier hopping between localized states. Evidence for the presence of a gap in the density of states leading to a transition to a more than half-filled band at temperatures above T_m was found in the thermopower results for samples with $x \sim \frac{1}{4}$. This may be due to on-site Coulomb repulsion. This and the resemblance between $\rho(T)$ for $x = \frac{1}{4}$ at high temperatures with that of $\rho(T)$ for CO-AFM $\text{Pr}_{0.5}\text{Sr}_{0.5}\text{MnO}_3$ (at low T), suggest that the samples with $x \sim \frac{1}{4}$ may be AF ordered at temperatures above T_c . Additional measurements are needed to find the evolution with temperature of the magnetic order for this composition.

The positive sign of S found in the FM state of most of the compounds studied is consistent with transport in a one-

electron band with polarized states. The small absolute values of S in a regime where the resistivity changes by orders of magnitude are worth noting. Various possibilities leading to such result are now under investigation.

Over wide ranges of temperatures in the FM state the semilog plots of ρ vs T look like plots of thermal expansion, including the anomalous thermal expansion around T_m . This supports the conclusion reached in Ref. 4 that in this regime the conductivity depends exponentially on the transfer integral, e.g., on W which in turn depends on temperature.

ACKNOWLEDGMENTS

We are grateful to E. Polturak (Technion) for drawing our attention to the manganese oxides, to M. Fibich and J. Genossar (Technion) for stimulating discussions and for some useful comments. We are grateful to R. Kalish (Technion) and S. Praver (Melbourne University) for discussions on the transport mechanism in Ref. 21. This research was supported by the Israel Science Foundation administered by the Israel Academy of Sciences and Humanities, and by the Fund for the Promotion of Research at Technion.

-
- ¹C. Zener, Phys. Rev. **82**, 403 (1951).
²P.-G. de Gennes, Phys. Rev. **118**, 141 (1960).
³J. H. Jonker and J. H. Van Santen, Physica **16**, 337 (1950).
⁴M. F. Hundley, M. Hawley, R. H. Heffner, Q. X. Jia, J. J. Neumeier, J. Tesmer, J. D. Thompson, and X. D. Wu, Appl. Phys. Lett. **67**, 860 (1995).
⁵R. von Helmolt, J. Wecker, B. Holzapfel, L. Schultz, and K. Samwer, Phys. Rev. Lett. **71**, 2331 (1993).
⁶V. Caignaert, A. Maignan, and B. Raveau, Solid State Commun. **95**, 357 (1995).
⁷J. Fontcuberta, B. Martinez, A. Seffar, S. Pinol, J. L. Garcia-Munoz, and X. Obradors, Phys. Rev. Lett. **76**, 1122 (1996).
⁸H. Y. Hwang, T. T. M. Palstra, S.-W. Cheong, and B. Batlogg, Phys. Rev. B **52**, 15 046 (1995).
⁹M. R. Ibarra, P. A. Algarabel, C. Marquina, J. Blasco, and J. Garcia, Phys. Rev. Lett. **75**, 3541 (1995).
¹⁰Y. Tomioka, A. Asamitsu, Y. Moritomo, H. Kuwahara, and Y. Tokura, Phys. Rev. Lett. **74**, 5108 (1995).
¹¹M. R. Lees, J. Barratt, G. Balakrishnan, D. McK. Paul, and M. Yethiraj, Phys. Rev. B **52**, R14 303 (1995).
¹²Y. Tomioka, A. Asamitsu, H. Kuwahara, Y. Moritomo, and Y. Tokura, Phys. Rev. B **53**, R1689 (1996).
¹³R. C. Miller, R. R. Heikes, and R. Mazelsky, J. Appl. Phys. Suppl. **32**, 2202 (1961).
¹⁴Note that in Ref. 13 the use of x is according to the formula $\text{La}_x\text{Ca}_{1-x}\text{MnO}_3$.
¹⁵A. Asamitsu, Y. Moritomo, and Y. Tokura, Phys. Rev. B **53**, R2952 (1996).
¹⁶M. Jaime, M. B. Salamon, K. Pettit, M. Rubinstein, R. E. Treece, J. S. Horwitz, and D. B. Chrisey, Appl. Phys. Lett. **68**, 1576 (1996).
¹⁷G. C. Xiong, Q. Li, H. L. Ju, S. N. Mao, L. Senapati, X. X. Xi, R. L. Greene, and T. Venkatesan, Appl. Phys. Lett. **66**, 1427 (1995).
¹⁸H. Kuwahara, Y. Tomioka, A. Asamitsu, Y. Moritomo, and Y. Tokura, Science **270**, 961 (1995).
¹⁹Y. Nishino, S. Inoue, S. Asano, and N. Kawamiya, Phys. Rev. B **48**, 13 607 (1993).
²⁰Strictly speaking since the extrapolation of $\rho(T)$ to $T=0$ is finite, the use of “insulatorlike” or “semiconductorlike” behavior is not appropriate to describe the temperature dependence in this regime.
²¹C. M. Hurd, J. Phys. C **18**, 6487 (1985).
²²D. Emin, Philos. Mag. B **52**, L71 (1985).
²³See, e.g., Fig. 20 in Chap. 6 in Charles Kittel, *Introduction to Solid State Physics*, 4th ed. (John Wiley, New York, 1971).
²⁴N. F. Mott and E. A. Davis, *Electronic Processes in Noncrystalline Materials* (Clarendon, Oxford, 1979).
²⁵ S_{sat} for $x > \frac{1}{2}$ could be very helpful in making one of the three possibilities preferable. However the three available plots in Ref. 13 for this regime (including CaMnO_3) show finite negative S at high T but not saturation.
²⁶G. Beni, Phys. Rev. B **10**, 2186 (1974).
²⁷Frank J. Blatt, *Physics of Electronic Conduction in Solids* (McGraw-Hill, New York, 1968), p. 211.